Aerodynamic Analysis of ANKA UAV and Heron UAV.

Conference Paper · April 2019

2 authors:

Seda Arabacı
cbü

Furkan Dilbaz

Aerodynamic Analysis of Anka UAV and Heron UAV

Seda KIRMACI ARABACI[1], Furkan DİLBAZ[1]

[1]Manisa Celal Bayar University, Department of Mechanical Engineering
Manisa/Turkey
*Corresponding Author: seda.kirmaci@cbu.edu.tr

Abstract

One of most important issue with in Unmanned Aerial Vehicles (UAV) is improvement of perpetuity capability which can be achieved by well designed aerodynamic shapes. The aerodynamic efficiency aims to good maneuverability and fuel saving. It is a superior feature that unmanned aircraft can be controlled by autonomous vehicles. It is preferred due to work with less energy consumption, low emission and noise levels and to be environmentally friendly. Compared to the aircraft, the production, use, maintenance and fuel costs of the UAVs are lower.

This paper investigates the shape of design and optimization for the improvement of aerodynamic performance. Tusaş Anka UAV and Israel Aerospace Industries (IAI) named Heron are compared. These forms were drawn in Solidworks 3D drawing program by the surface knitting process. And then they were analyzed by using Ansys FLUENT program. The drag coefficient of the Anka UAV is 7.6 % lower than Heron UAV at 217 km/h. The Heron UAV lift coefficient is 65 % lower than Anka UAV. Anka UAV has more fuel savings than Heron UAV.

Keywords: UAV, ANKA, Heron, Aerodynamics, Computational Fluid Dynamics, drag coefficient

Introduction

The range of unmanned aerial aircraft (UAV) was continuously developing. New constructive solutions from small to mass size which were comparable to piloted aircraft. The main reason of UAV use was due to lower cost of design, realization and operation (on flight hour) in comparison with human piloted aircraft. (Pepelea et al., 2016) The aerodynamic design of a low-cost UAV able to perform aerial surveillance of volcanic environments were researched by Bravo-Mosquera et al. Its main mission was to transmit real time volcanic data to a remote location, in order to aid to forecast volcanic eruptions, as well as avoiding the exposition of pilots and scientists to these dangerous flight conditions. An approximation of the numerical results with the experimental ones was obtained, where the C_D values at zero angle of attack were 0.048 and 0.053 respectively. The high turbulence above the craters produced substantial performance reductions, resulting in the movement back. (Bravo-Mosquera *et al.*,

2017) Analytical and computational methods were used to design the adaptive multi winglet device, which was composed by three winglets with its own geometry fitted. Six configurations were created by modifying only the cant angle of each winglet in order to determine the arrangement that provides the best aerodynamic characteristics through a study of CFD, using the Reynolds–Averaged–Navier–Stokes (RANS) equations coupled with the Shear Stress Transport (SST) turbulence model. A non-structured mesh around the entire external geometry was generated consisting of 11.2 million of computational elements. The optimal concept of the AG-Nel 25 aircraft present smaller vortices formed at the tip in comparison with the baseline concept. (Bravo-Mosquera *et al.*, 2018) The performance specifications were compared with a conventional UAV platform to point out the main advantages and disadvantages of the BWB for MALE UAV applications. When compared to a conventional UAV configuration the difference in aerodynamic efficiency was at the order of magnitude of 30%. (Panagiotou, Fotiadis-Karras & Yakinthos, 2018) The article showed a case of numerical analysis of the lifting surface on the UAV type flying wing. The results of the simulation of flow around the carrying capacity surface for the flying type wing was affected by two main factors, as follows: the first was the nature and quality (density) of the mesh network and the second was the quality of turbulent flow model used. (Vasile, 2016) Under secretariat for Defense Industries (SSM) Mini needed in Turkey's UAV system was classified as tactical and MALE and launched development projects for each class. Preparations were planned for emergency needs. TAI, having acquired significant experience in the past, was assigned to develop the MALE class UAV platform. The TIHA, or Anka, which was developed for this purpose, competes with the examples abroad, such as 24 hours aerial stay, altitude of 9000 meters (Altunok, 2010). In this paper, the aerodynamic characteristics such as lift coefficient, drag coefficient are obtained and compared. In addition, the CFD visualization of flow and pressure distribution on the surface of the The Tusaş Anka UAV and Israel Aerospace Industries (IAI) named Heron model had been plotted to analyze the flow behavior.

Material and Method

Medium Altitude Long-Aerial Tusaş Anka UAV night and day, including bad weather conditions, exploration, surveillance, fixed / moving target detection, diagnosis, identification and tracking purposes, real-time image intelligence was being developed for tasks. (Tai, 2019) Heron is a medium altitude, long endurance UAV system primarily designed to perform strategic reconnaissance and surveillance operations. It is design and manufactured by Israel Aerospace Industries (IAI) at its Malat division, Israel, in partnership with the Canadian company MacDonald, Dettwiler and Associates (MDA). The Australian Department of Defence (DoD) awarded the Heron systems contract to MDA. (AirForce Technology, 2019) Anka UAV and Heron UAV were created as drawn in Solidworks and simulated with computational fluid dynamics. Models was formed by surface coating and then drawings were transformed into one piece solid model. Anka UAV and 3D model shown in Figure 1, Heron UAV and 3D model shown in Figure 2.

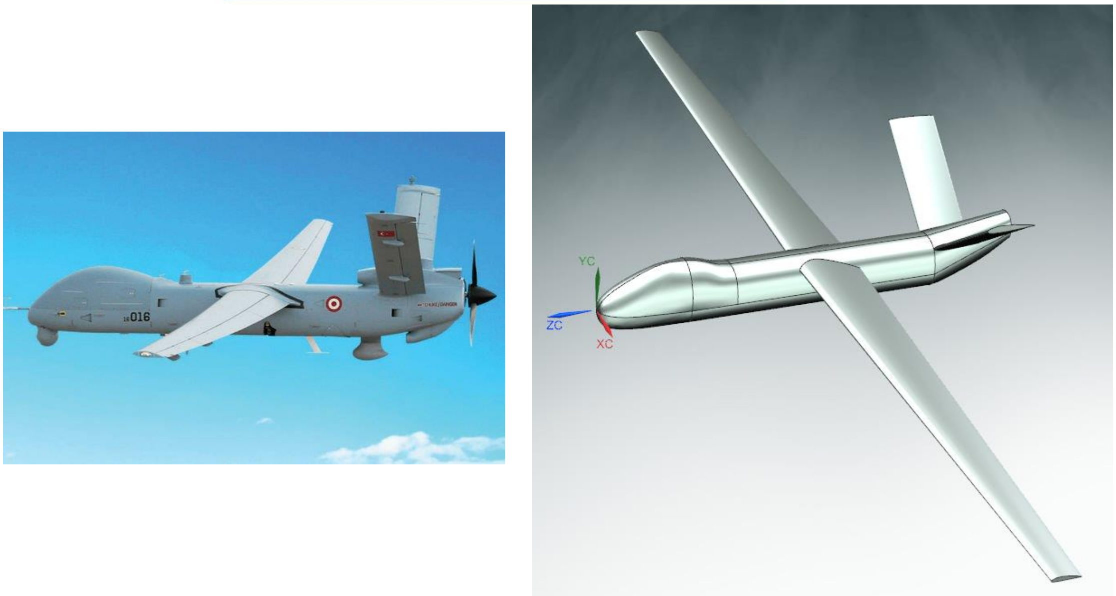

Figure 1. Tai-Anka UAV and 3D model

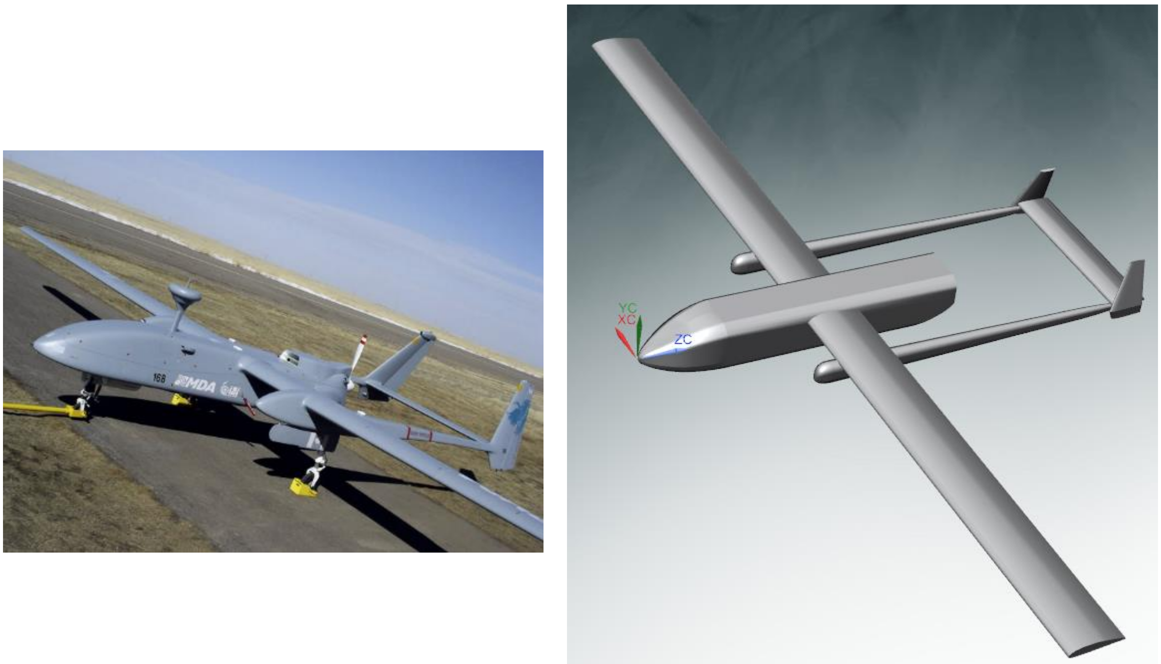

Figure 2 Heron UAV and 3D model

The dimensions of the models are given in Table 1.

Table 1. UAV general features (Tai, 2019)

UAV general features	Tai-Anka UAV	Heron UAV
Crew	None	None
Wingspan [m]	17.3	16.6
Length [m]	8	8.5
Wing area [m^2]	13.8	13
Total take-off weight [kg]	1500	1150
max speed [km/h]	217	232

The dimensions of the computational domain and the boundary conditions were adjusted to the characteristics and location of the control volume used for the analysis. Simulations were performed with the ANSYS Fluent, resolving k-ω model, coupled with the Shear Stress Transport (SST) turbulence model. It was observed that the k-ω SST model performs better in areas with flow separation than other turbulence models. (Menter, 1993)

Numerical Methods

The models were located in a control volume. The dimensions of the computational domain were 40 m, 28 m and 88 m in Ansys Workbench. The models were replaced in the control volume with 3 the UAV length from the inlet, 6 times UAV length from the outlet and 2.5 times the UAV width from sides. And a box was created for smooth mesh.
Another important factor in improving the quality of the mesh structure was the effect of the boundary layer thickness. The boundary layer thickness determined as the inflation in the analysis was calculated by the equation used by NASA.

$$C_f = 0{,}058(R_e)^{-0{,}2} \quad (1.1)$$

$$\tau_w = 0{,}5\rho C_f V^2 \quad (1.2)$$

$$U_* = \sqrt{\frac{\tau_w}{\rho}} \quad (1.3)$$

$$y = \frac{y^+\mu}{U_*\rho} \quad (1.4)$$

As a result of these equations, the Reynolds number was calculated primarily to find the boundary layer thickness. The parameters were where C_f was the skin friction, τ_ω was the wall shear stress, U^* was the friction velocity. In the aerodynamic analysis, the reference displacement should be $y^+ \leq 1$. (Frank et al.,2013) In this paper, $y^+=1$ was used and the turbulence model was selected as k-ω SST model which was recommended for external flow. First boundary layer thickness *y* was found by taking $y^+=1$.

The Navier-Stokes equations were solved, assuming incompressible flow and steady state. Independence mesh analysis was carried out in order to achieve the best precision in the results.

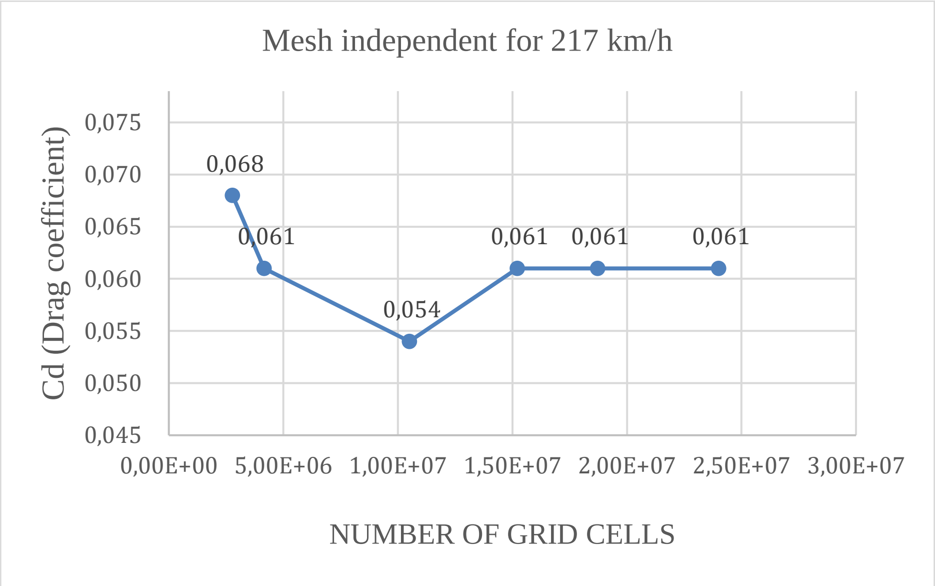

Figure 3. Mesh Independent for 217 km/h

Figure 3 gave the size of the mesh elements of the cell grid. It had been observed that from a domain with 15 million of elements (mesh independence criteria) and the results showed that Cd didn't change after 15 million mesh. Therefore, this number of elements was chosen as the converged for this study. 18e106 tetrahedral elements were used for Anka UAV meshing and the C_L and C_D coefficients were calculated in a y+ ≈ 1. The first layer thickness of mesh cells away from the wall was set in y = 6.41e-6 for UAVs. Figure 4 showed the final grid formation, and the mesh quality was found to be acceptable.

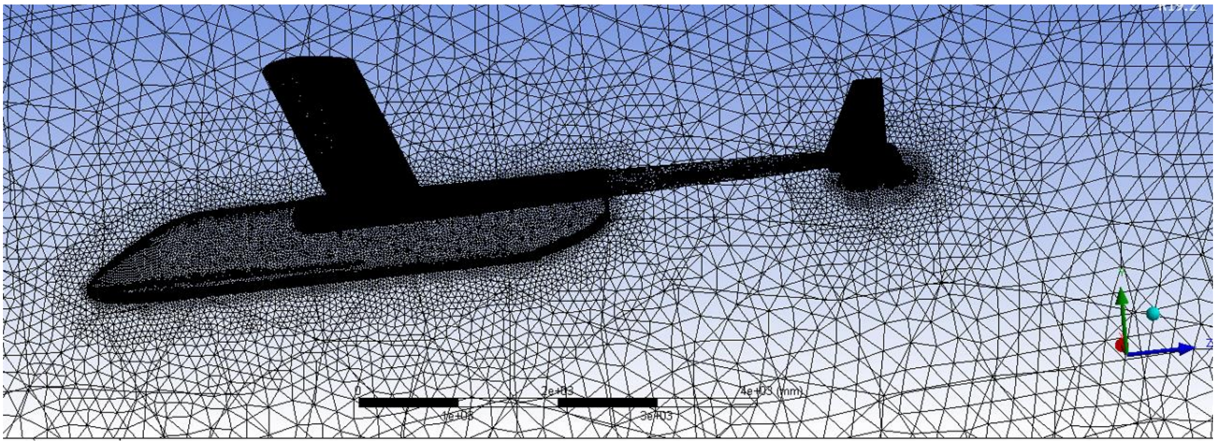

Figure 4. Final mesh of UAV

The average orthogonal quality was 0.86, average skewness was 0.13 which should be acceptable from the ANSYS quality requirements. The present values of mesh were considered to be acceptable. (Djojodihardjo, Ahmed & Yousefian, 2014)

The boundary conditions were determined, velocity was set at 217 km/h at the inlet surface, zero pressure at outlet, no slip condition at the UAV, free slip condition at the sides for models. The temperature, density of air and dynamic viscosity values used in the analysis were taken as 15.5°C, 1.225 kg/m^3 and 1.79 x 10^{-5} kg/ms, respectively, which represents the study Reynolds number approximately equal to which calculated this study Reynolds number approximately equal to 3.45e6 for Anka UAV, and 4.13e6 for Heron UAV. Inlet turbulence intensity equal to 2.5 % and hydrolic diameter 33 m also calculated. It was chosen for low altitude flight regimes. Symmetry condition was imposed in the half of the along the axis plane of the model. Range of angle of attack was examined at α =0◦. The convergence reached with 1000 iterations in CFD.

Research Findings and Discussion

In this section, the aerodynamic characteristics of the analytical for the UAVs were analyzed and compared. The variables were: C_L, C_D and drag force which affecting aerodynamic properties were determined. According to the results of Table 2, for at 0° of attack contained of Heron, +4° of attack contained of Anka UAV.
The drag coefficient of the Anka UAV was found to be 7.6 % lower than Heron UAV at 217 km/h. Anka UAV is more fuel savings than Heron UAV. Factors affecting the drag force; The square of the velocity of the UAV was directly related to the density of the air, the geometry and area of the wing profile.

Table 2. Aerodynamic results of UAVs at 217 km/h

Model	Drag coefficient (C_D)	Drag Force [N]	Lift coefficient (C_L)
Anka UAV	0.061	739.67	0.99
Heron UAV	0.066	808.83	0.35

The lift coefficients were investigated, and the lift coefficient of Heron UAV was 65 % lower than Anka UAV model. The high lift coefficient means that the Anka has a high load bearing capacity. It was seen in the analyzes that the maximum speed on the wing profile of Heron was 93 m/s, while the maximum speed on the wing profile of the Anka UAV was 88 m/s. Velocity and pressure were seen Table 3.

In the analyzes, while Anka UAV had an attack angle of $+4^0$, Heron UAV 0^0 had an attack angle. The magnitude of the angle of attack was closely related to the lift force of the wing.

This difference in the angle of attack had made this difference between the lift coefficients of both Anka and Heron. Since the wing profile used in both models was NACA 4415, drag and lift coefficients of this profile are given in 0^0 and 4^0; at 0^0; C_L= 0.3995, C_D= 0.00817; at 4^0; C_L= 0.8799, C_D= 0.00838 for NACA 4415 wing profile (Airfoiltools, 2018).

The difference in the angle of attack did not affect the comparability of drag forces in this study because there was not much difference between drag coefficients.

Table 3. Velocity and pressure of UAVs

Model	max. Velocity (m/s)	max. Pressure (Pa)
Anka UAV	88	2243
Heron UAV	93	2205

The biggest reason for this result was the pressure difference in the wings. Anka UAV and Heron UAVs' maximum pressure was 2243 Pa and 2205 Pa, respectively.

As seen from the Figure 5, velocity distribution, flow separation were occured. The air velocity on the upper surface of the Anka UAV was higher than the other surfaces. In this case, a pressure difference could be occur due to the speed differences. This pressure difference also constituted the lift force.

The airflow from the upper and lower surfaces of the aerofoil converged at the trailing edge and flows backwards with a slight separation. This process reduced the pressure on the trailing edge, which created an increase in the favorable pressure gradient on the upper surface of the aerofoil. The disappearance of flow separation, the backward shift of the stagnation point and the acceleration of the flow velocity of the aerofoil upper surface increased the circulation and lift of the aerofoil. A large degree of flow separation occured in the trailing edge of the UAVs, resulting in a large vortex.

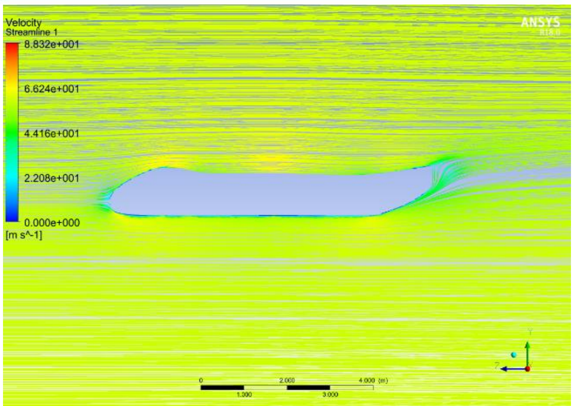

Figure 5. Velocity and streamline of Anka UAV at 217 km/h

As seen from the pressure distribution, the pressure in the lower part of the body was higher compared to the pressure acting on the upper part. In addition, the high pressure zones were located in the region near the edge of the attack and in the front part of the body and were 2243 Pa shown as Figure 6.

Velocity and streamline of Heron UAV were seen Figure 7. Pressure of Heron UAV at 217 km/h was 2205 Pa in Figure 8.

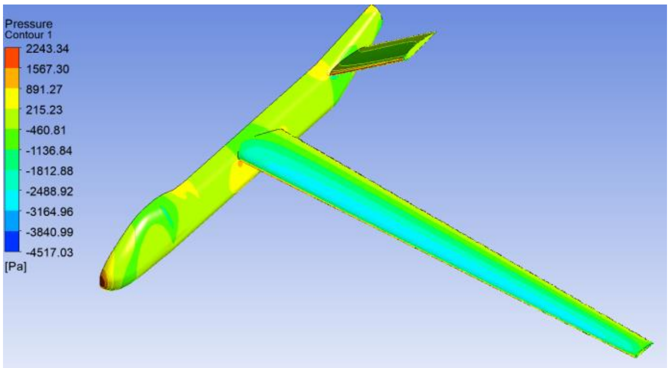

Figure 6. Pressure of ANKA UAV

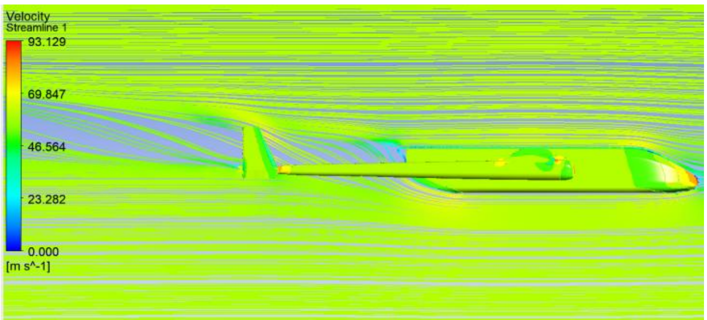

Figure 7. Velocity and streamline of Heron UAV

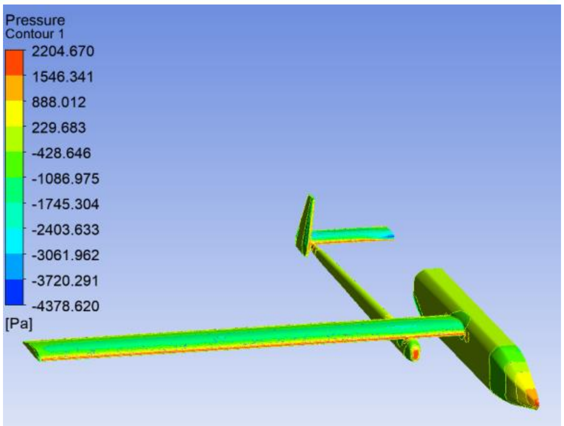

Figure 8. Pressure of Heron UAV

Results and Suggestions

This paper represents the fuel consumptions depending on shape. Aerodynamics properties of Anka UAV compared with the Heron UAV. The above analysis shows the aerodynamic characteristics for a UAV obtained through 3D drawn and simplified geometry in zones. For a better analysis, it is necessary a finer mesh, which is suitable for RANS.

The results of the simulation of flow around the UAV surface for the flying type wing is affected by two main factors, as follows: the first is the quality and density of the mesh parameter and the second one is the model of turbulent flow. A comparison numerical results based on distribution of the velocity vector and distribution of the Reynolds tensor is required. The drag coefficient Anka UAV was found to be 0.061, Heron was 0.066. According to the Heron UAV, the drag force was 8.6 % and the drag coefficient improved by 7.6 %. The lift coefficient of Heron UAV was 65 % lower according to Anka UAV model.
According to these results fuel consumption of Anka UAV is better then Heron UAV because of drag coefficient.

Delaying the flow seperation is recommended to improve the wing. It can be done by changing the airfoil of the wing with more appropriate airfoil for low speed, or by increasing the surface area of the wing to generate more lift, or by twisting the wing to delay the separation. This represents the optimum flight configuration with optimum fuel consumption.

References

Air Force Technology, 2019. Title of Topic, https://www.airforce-technology.com/projects/heron-uav/, Accepted Date: 10.01.2019

Airfoiltools, 2018. http://airfoiltools.com, Accepted Date: 10.6.2018.

Altunok, T., 2010, Development of Unmanned Aerial Vehicles, Science and Technology, 517, 28-31.

Anonymous, 2015. Title of Topic, www.globalwarming.com , Accepted Date: 15.10.2018

Ansys Fluent User's Guide 14, 2011, 2948p

Bravo Mosquera P.D., Botero Bolivar L., Acevedo Giraldo D., Ceron-Munoz H.D., 2017. Aerodynamic Design Analysis of a UAV for Superficial Research of Volcanic Environments. Aerosp. Sci. Technol., 70600-614.

Bravo Mosquera P.D., Ceron-Munoz H.D., Díaz-Vazquez G., Martini Catalano F., 2018. Conceptual design and CFD analysis of a new prototype of agricultural aircraft. Aerosp. Sci. Technol., 80156-176.

Canan, C., 2005. Agricultural Rycle, Applied Science Institute, PhD Thesis, Turkey

Djojodihardjo, H., Ahmed, R.I., 2014. An Analysis on the Lift Generation for Coanda Micro Air Vehicles, IEEE, ICARES Conference Proceeding, Yogyakarta, Indonesia.

Frank T., Gerlicher B., Abanto J., 2013. Drivaer Aerodynamic Investigations, USA for a New Realistic Generic Car Model using ANSYS CFD, ANSYS Inc Tutorial, Germany.

Menter, R., 1993, Zonal Two Equation k-ω Turbulence Models for Aerodynamic Flows, 24th Fluid Dynamics Conference, Orlando, Florida

Panagiotou P., Fotiadis Karras S., Yakinthos K., 2018. Conceptual Design of a Blended Wing Body Male UAV, Aerosp. Sci. Technol., 7332-47.

Pepelea D., Cojocaru M. G., Toader A., Niculescu M. L., 2016. CFD Analysis for Uav of Flying Wing, Sci. Res. Educ. Air Force, 18 (1): 171-176.

Tai, 2019. Title of Topic, https://www.tai.com.tr/urun/anka, Accepted Date: 10.01.2019

Vasile P., 2016. CFD Analysis of UAV Flying Wing, Incas Bull., 8 (3), 65-72.